scientific reports

Check for updates

OPEN

Optimization of machining parameters for turning operation of heat-treated Ti-6Al-3Mo-2Nb-2Sn-2Zr-1.5Cr alloy by Taguchi method

Ramadan N. Elshaer[1]✉, Ali Abd El-Aty[2,3], Esraa M. Sayed[2], Azza F. Barakat[2] & Arafa S. Sobh[2,4]

TC21 alloy is a high-strength titanium alloy that has been gaining attention in various industries for its excellent combination of strength, toughness, and corrosion resistance. Given that this alloy is hard to cut material, therefore this study aims to optimize the process parameters of Turing this alloy under different conditions (i.e. as-received alloy, and heat-treated alloy). The L9 Taguchi approach-base orthogonal array is used to determine the optimum cutting parameters and the least number of experimental trials required. The achievement of this target, three different cutting parameters are used in the experimental work; each cutting parameter has three levels. The cutting speeds are chosen as 120, 100, and 80 m/min. The feed rates' values are 0.15, 0.1, and 0.05, mm/rev, and the depth of cut values are 0.6, 0.4, and 0.2 mm. After applying three steps of heat treatment (First step: is heating the sample to 920 °C for 1 h then decreasing to 820 °C also for 1 h, second step: cooling the sample to room temperature by water quenching (WQ), the third step: holding the sample at 600 °C for 4 h (Aging process)). The results revealed that the triple heat treatment led to the change in the microstructure from (α + β) to (α + β) with secondary α platelets (α_s) formed in residual β matrix leading to a decreased surface roughness by 56.25% and tool wear by 24.18%. The two most critical factors that affect the tool insert wear and surface roughness are the death of cut and cutting speed, which contribute 46.6% and 46.7% of the total, respectively. Feed rate, on the other hand, has the least importance, contributing 20.2% and 31.9% respectively.

Keywords Heat treatment, Turning parameters, TC21, Wear of tool insert, Surface roughness

Nowadays, Titanium alloys are significant in a variety of domains and uses. Because of their high ratio of strength to weight, titanium alloys have a significant contribution, especially in the trials in biomedical, aerospace, automotive, and communication engineering. Titanium alloys have a series of grades such as Ti555.3, Ti6Al4V, and their new versions like TC21 alloy[1–3].

The TC21 alloy represents a new version of titanium alloys, characterized by its chemical composition of Ti-6Al-3Mo-2Zr-2Sn-2Nb-1.5Cr-0.1Si. This alloy features a dual-phase (α + β) microstructure, making it versatile for various applications, either as-received or heat-treated[4]. It exhibits high tensile strength and toughness, even at elevated temperatures, and despite its lightweight, it offers substantial corrosion resistance[5]. Although TC21 is a promising material for diverse applications including military, automotive, aerospace, biomedical devices, sports cars, and high-end sporting goods and consumer electronics, its implementation is hindered by high raw material costs and its challenging machinability[6]. These factors contribute to poor surface quality, reduced machining efficiency, and accelerated tool wear[7]. Consequently, there is a significant need for in-depth research into the machining processes for this alloy. Previous studies have explored the turning process of TC21 Ti-alloy, highlighting these challenges[5–7].

[1]Tabbin Institute for Metallurgical Studies, Cairo, Egypt. [2]Mechanical Engineering Department, Faculty of Engineering, Helwan University, Cairo, Egypt. [3]Mechanical Engineering Department, College of Engineering et al Kharj, Prince Sattam Bin Abdulaziz University, 11942 Al Kharj, Saudi Arabia. [4]School of Engineering and Applied Sciences, Nile University, Giza, Egypt. ✉email: ramadan_elshaer@yahoo.com

Over the last few decades, the determination of cutting parameters has been a major challenge, traditionally addressed using full factorial methods, which are both costly and time-consuming[8]. Recent advancements in parameter selection techniques have led to the development of more efficient methods to identify optimal machining parameters[9]. Among these methods are ANOVA, Taguchi, Artificial Neural Network (ANN), and Response Surface Methodology (RSM)[10–15]. As new titanium alloys like TC21 Ti-alloy are developed, it becomes crucial to study their performance in various applications. This includes examining how the TC21 Ti-alloy behaves in metal forming, how cutting parameters and microstructure are affected by heat treatment, and its overall machinability, particularly in processes such as turning, milling, and turn-milling, where machinability remains a significant challenge[11,12].

The mechanical properties of the TC21 Ti-alloy surpass those of Ti6Al4V and Ti555.3 alloys, leading to its application in various critical fields. Nevertheless, the primary challenge with this alloy is its difficult machinability[13]. Numerous studies have focused on this issue, employing a range of machining parameters to conduct turning operations[10–16]. These studies have predominantly optimized the turning cutting conditions using the Taguchi method. Additionally, some researchers have utilized the full factorial technique along with the fractional factorial approach of the Taguchi method[16]. The findings of these investigations indicate that the Taguchi method, compared to the full factorial method, is more suitable for evaluating the machinability of materials that are difficult to cut.

Isothermal tensile tests were used in various investigations to analyze the deformation behaviour of the TC21 alloy, using stress–strain curves to determine that flow stress inversely correlates with temperature, while maintaining a direct relationship with strain rate[17–22]. In parallel, other studies employed constitutive modeling and high-temperature tensile tests under hot deformation conditions, identifying a direct link between strain and stress, and an inverse relationship between flow stress and strain rate[18]. Additional research focused on the effects of tool microstructure and variations in tool rake angle on the machinability of TC21 Ti-alloy[19]. Using finite element analysis, these studies assessed the cutting performance of the alloy, while turning operations were simulated using the Johnson–Cook (JC) technique and 3D finite element analysis[20]. The findings indicated that adjustments to the tool rake angle decreased scrape serration, reduced wear on the tool insert, and enhanced the machining efficiency of the alloy. However, it is noted that 3D simulations are highly reliant on experimental data, indicating certain limitations in their application.

In addition to turning studies, various milling studies utilized three distinct methods to investigate the cutting forces involved[23–26]. These studies analyzed the impact of cutting forces, the temperature during cuts, and the lifespan of milling cutters in relation to milling parameters, wear of the milling cutter, and the material of the tool[23]. Results indicated that cutting forces, the degree of cutting heat, and the life of the cutter significantly affect the tool material, wear, and milling parameters[24]. Concurrently, some researchers focused exclusively on how milling parameters influenced cutting forces, temperatures, and tool life[25]. Additionally, under different machining conditions, the wear on titanium, aluminum, and nitrogen-titanium-nitride-coated carbide tools, as well as the deposition from physical vapor, were examined[26]. The findings highlighted a strong relationship between increases in tool wear and the magnitude of the cutting force increment.

The Response Surface Methodology, along with the Taguchi technique, has been used to optimize cutting conditions. This methodology helped in developing models to predict surface roughness, demonstrating that the primary objective of optimization is to maximize the material removal rate. Additionally, a combination of response surface methodology and genetic algorithms was utilized to fine-tune the machining parameters. Surface roughness values were determined by averaging measurements from three different areas on the workpiece's surface[27].

In this study, the Taguchi method was applied using Minitab 19 to optimize turning parameters and identify ideal conditions that minimize surface roughness and tool insert wear. Subsequently, the ANOVA method was used to pinpoint the most critical parameters. Given the demanding machining requirements of the TC21 Ti-alloy, a tungsten carbide-coated cutting tool (DCMT 11 T 304-NF NS 4125) was employed. The machining process was conducted twice to ensure reliability in the results, and the average of the two responses was calculated.

Material and method

Material description, heat treatment stages, experimental equipment, cutting tool, and measuring tools

The materials used in this study is TC21 Ti-alloy, which has a microstructure made up of two phases ($\alpha+\beta$) and a chemical composition of Ti—6Al—3Mo—2Nb—2Sn—2Zr—1.5Cr as received[28]. The as-received sample is treated in three stages: first, it is heated to 920 °C for an hour and then cooled to 820 °C for an hour; second, water quenching (WQ) is used to cool it to room temperature; and third, it is aged for four hours at 600 °C as shown in Fig. 1. This triple heat treatment transformed the microstructure of the TC21 alloy from an ($\alpha+\beta$) structure to a new ($\alpha+\beta$) structure with the formation of secondary α platelets (αs) within the remaining β matrix as shown in Fig. 2. The transformation of the microstructure from ($\alpha+\beta$) to ($\alpha+\beta$) with αs platelets is believed to be responsible for the observed enhancements in hardness and strength of the material. Therefore, there were an increase in the material's hardness and strength: the hardness of the heat-treated TC21 alloy increased significantly, rising 44.63% to 50.33 HRC, and the heat treatment improved the TC21 alloy's overall strength in addition to increasing its hardness.

Turning experiments were carried out on CNC machine with a maximum spindle speed of 3000 rpm, known as GOOD WAY to machine the TC21 alloy sample, which had a length of 110 mm and a diameter of 33 mm. The machining process involved conducting 9 separate experiments, with each experiment performed on a 5 mm length section along the sample's total length as shown in Fig. 3. The three key experimental parameters are cutting speed, feed rate, and cutting depth. The surface roughness of the TC21 Ti-alloy specimen was assessed using

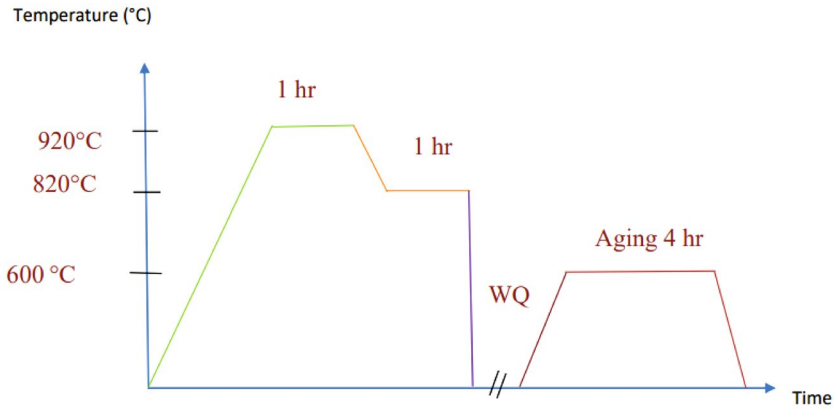

Figure 1. Heat treatment cycle.

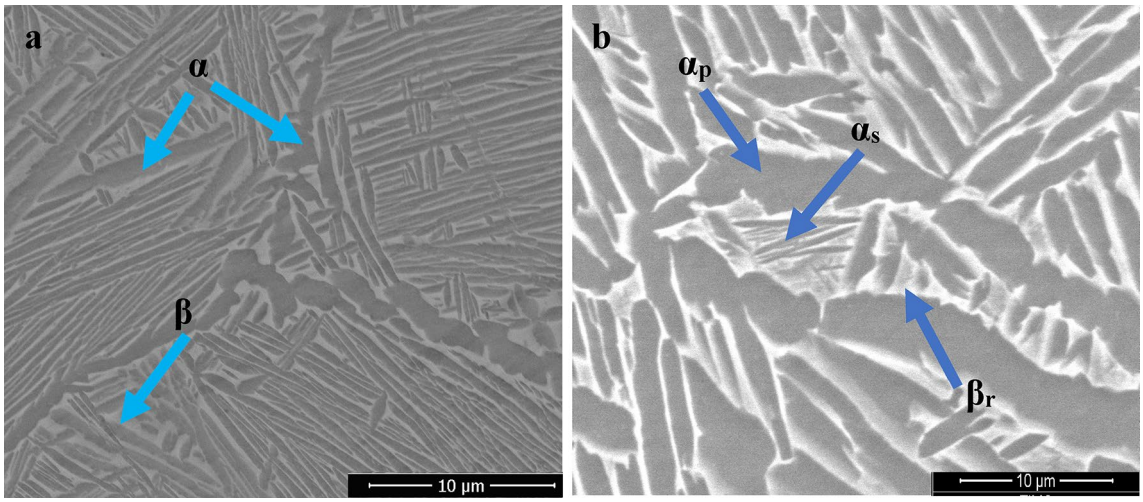

Figure 2. The Microstructure of (**a**) initial and (**b**) heat-treated alloy.

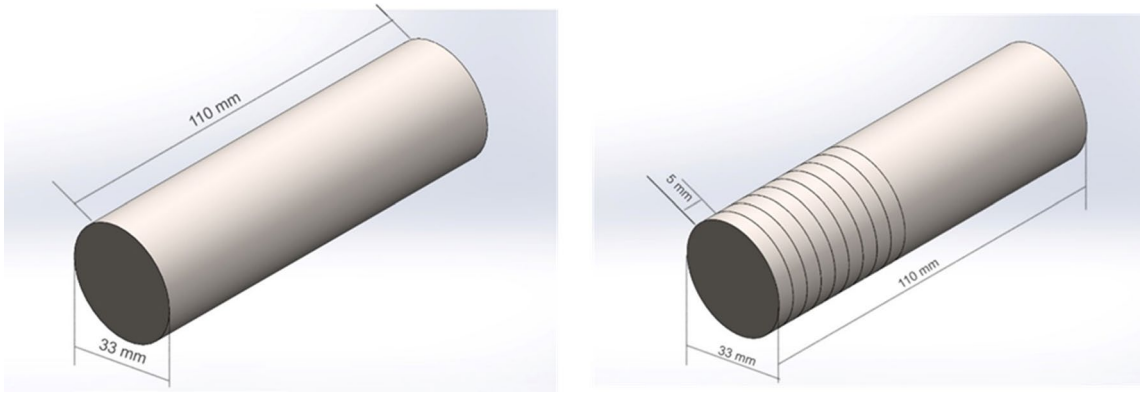

Figure 3. Work sample.

the DIAVITE DH-5 surface roughness tester, with the surface roughness value (Ra) representing the average taken from three different surface locations. Due to the challenging nature of machining materials like TC21, indexable tungsten-coated carbide cutting tools (DCMT 11 T 304-NF NS 4125) with a 0.4 mm nose radius are employed. Additionally, tool wear for these inserts was examined using scanning electron microscopy (SEM).

Experimental design via the Taguchi approach

The Taguchi method utilizes a fractional factorial design to decrease the total number of experiments needed. An orthogonal array L9 was used to conduct experiments for three parameters (feed rate, cutting depth, and speed of cut), where each tested at three distinct levels (levels 1, 2, and 3). The specific levels and the layout of the orthogonal array for these parameters are detailed in Tables 1 and 2.

These parameters were chosen with the understanding that the cutting speeds needed to machine titanium alloys exceed 54 m/min, with the majority of researchers employing speeds between 80 and 160 m/min. Because titanium alloys are used in small applications, there are small cutting depths within the scope of 0.1: 1 mm in addition to the cutting speed range. These specifications were chosen to make the machining process easier for material that is challenging to cut (TC21 Ti-alloy).

Parameter optimization for a given process is the first step in the Taguchi technique, which improves quality performance and reduces experimental turning costs. Process parameters are optimized by the Taguchi technique, which produces ideal parameters that are not affected by noise or external circumstances. The Taguchi method employs a loss function to measure the deviation between the desired value and the experimental results. A signal-to-noise (S/N) ratio is further converted from this loss function.

The required response category determines the signal-to-noise (S/N) ratio. The signal-to-noise ratio (S/N) can be computed using one of three formulas. Equation (1) indicates that smaller is better (SB), Eq. (2) indicates that nominal is better (NB), and Eq. (3) presents larger is better (LB)[29,30].

The smaller is the better (minimize):

$$S/N = \eta = -10\log 10\left(\sum \left(Y^2\right)/n\right) \tag{1}$$

Nominal is best

$$\mathrm{S/N} = \eta = 10log10\left(\frac{\overline{Y}^2}{S^2}\right) \tag{2}$$

Larger is better (maximize)

$$\mathrm{S/N} = \eta = -10log10\left(\Sigma\left(\frac{1}{Y^2}\right)/n\right) \tag{3}$$

To verify the precision of the DIAVITE DH-5 tester and scanning electron microscope (SEM), a calibration stage was established using an international standard block. Three tests were conducted to calculate the average response for the surface roughness measurements.

Results and discussion

Surface roughness

The analysis of ratio of signal to noise

In this study, higher effectiveness is demonstrated by lower surface roughness (Ra) values. For optimizing surface roughness, the "smaller is better" approach was adopted to identify the best machining parameters. The

Factors	Level (1)	Level (2)	Level (3)
Speed of cut V(m/mm)	80	100	120
Feed rate f (mm/rev)	0.05	0.10	0.15
Cutting depth a (mm)	0.2	0.4	0.6

Table 1. Parameters and Their Corresponding Levels for the Study.

Exp. No	Cutting speed (V)	Feed rate (f)	Cutting depth (a)
1	1	**1**	**1**
2	1	2	2
3	1	3	3
4	2	**1**	3
5	2	2	**1**
6	2	3	**2**
7	3	**1**	2
8	3	2	3
9	3	3	**1**

Table 2. L9 Orthogonal Array using the Taguchi Method.

optimal levels of machining parameters are those with the highest signal-to-noise ratio (S/N). Table 3 presents the calculated S/N ratios for each parameter level. The experiment with the highest S/N ratio, experiment no. 9 (V3 f3 a2), was identified as providing the ideal surface roughness parameters, with settings of V = 120 m/min, f = 0.15 mm/rev, and a = 0.4 mm. Table 4 details the best-performing parameters.

For each parameter, the average signal-to-noise (S/N) ratio is calculated to rank the cutting parameters by their importance. For instance, Equations (4-6) illustrate the method for calculating Factor V (cutting speed)[31]:

$$SNv_1 = (3.0568 + 15.5630 + 3.2230)/3 = 7.281 \tag{4}$$

$$SNv_2 = (7.0003 + 4.0132 + 14.2739)/3 = 8.429 \tag{5}$$

$$SNv_3 = (3.1812 + 17.9468 + 23.0980)/3 = 14.742 \tag{6}$$

The range is determined in order to calculate the effect of this factor:

$$\Delta = SNV_{max.} - SNV_{min.} = 14.742 - 7.281 = 7.461 \tag{7}$$

According to Table 5 in this study, the cutting depth parameter has the biggest variation between its levels and, as a result, has a significant impact on the experiment response (surface roughness), while the cutting speed parameter has less of an impact.

The variation for all parameters with signal-to-noise ratio is displayed in the following figure. The delta values for parameters V, f, and an are 7.461, 9.119, and 11.748, respectively, as shown in Table 5. Figure 4 plots the delta value for each parameter[32–38].

From Fig. 5, it is shown that the surface roughness value is in direct relation to the cutting speed parameter that decreases when cutting speed and feed rate increase. Still, it decreases from level one to level two and then increases from level two to level three with increasing depth of cut. It is noticed that there is a long variation between the levels of each of the two parameters (depth of cut and feed rate). Consequently, the mentioned two parameters occupy the first two affected parameters on the machining process. Therefore, the cutting speed is at the last affected parameter in the machining process.

Experimental serial number	Speed of cut V (m/min)	Feed rate f	Depth of cut a (mm)	Surface roughness Ra (µm) Mean	Ra S/N (um)
1	SO	0.05	0.2	0.703333	3.0568
2	80	0.10	0.4	0.166667	15.5630
3	80	0.15	0.6	0.690000	3.2230
4	100	0.05	0.4	0.446667	7.0003
5	100	0.10	0.6	0.630000	4.0132
6	100	0.15	0.2	0.193333	14.2739
7	120	0.05	0.6	0.693333	3.1812
S	120	0.10	0.2	0.126667	17.9468
9	120	0.15	0.4	0.070000	23.0980

Table 3. Surface Roughness (Ra) Experimental Results.

Exp. No	Process parameters	Surface roughness (µm)
2	V_3 f_3 B2	0.07

Table 4. Optimal Process Parameters.

Level	V	F	A
1	7.281	4.413	11.759
2	S.429	12.50S	15.220
3	14.742	13.532	3.472
Delta	7.461	9.119	11.748
Rank	3	2	1

Table 5. Signal-to-Noise (S/N) Response and Delta Value for Each Parameter.

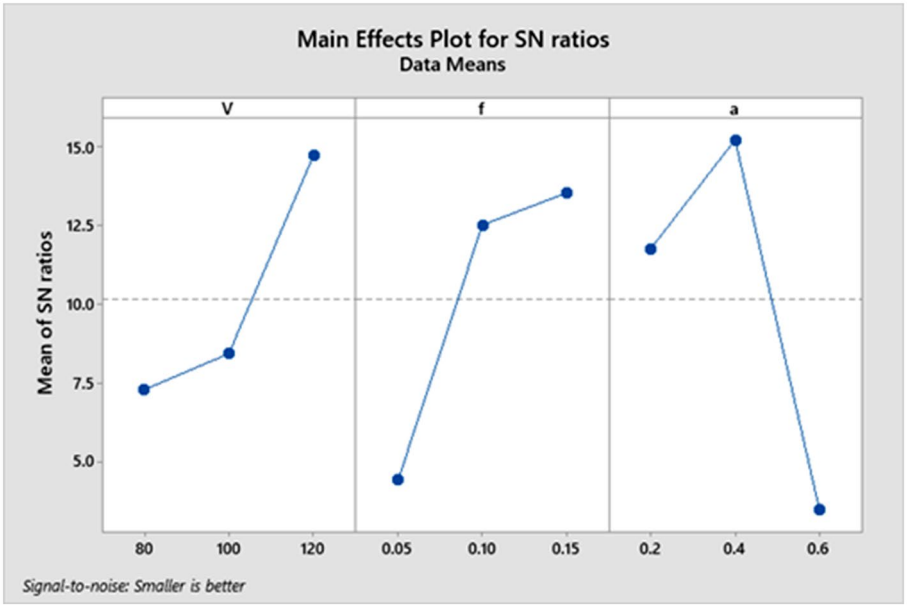

Figure 4. Average Signal-to-Noise (S/N) Ratio for Surface Roughness (Ra).

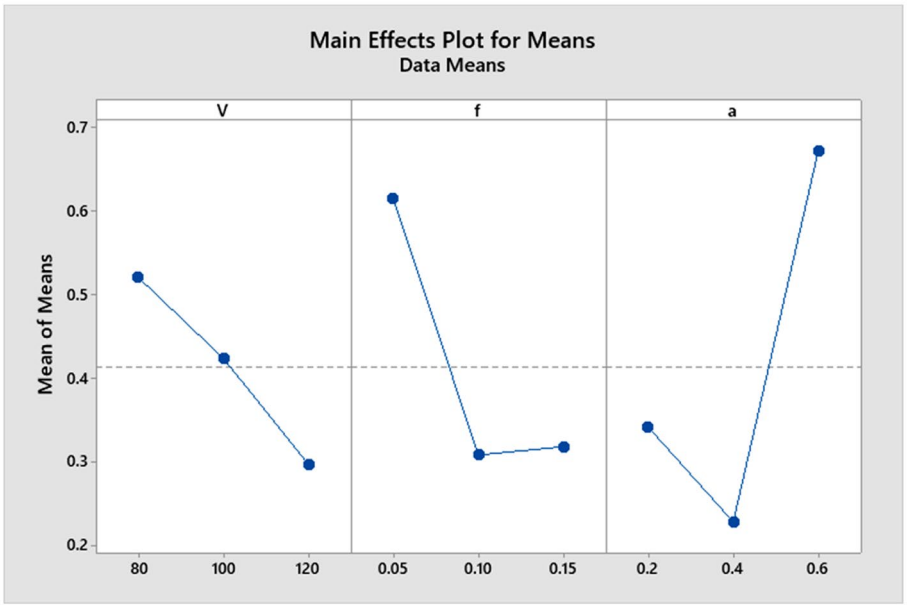

Figure 5. Main effects plot for means for Ra.

Variance Analysis (ANOVA)
ANOVA was employed to assess the effects of cutting depth, feed rate, and speed on surface roughness. The results are presented in Table 6, with a confidence level of 95%. Cutting depth was identified as the most influential factor, contributing 46.6% to the variability in surface roughness. Conversely, cutting speed was the least significant parameter, accounting for only 20% of the variation. All parameters were deemed significant in the machining process, as indicated by their P-values being lower than 0.05.

Tool wear

The analysis of ratio of Signal to noise
Greater effectiveness in this work is indicated by decreased tool wear. To achieve the best machining parameters, the smaller-is-better approach to tool wear was chosen. An ideal level is represented by the machining parameter levels that have the highest signal-to-noise ratio (S/N). Table 7 shows the computed (S/N) ratio for each parameter level. Using the S/N ratios, experiment no. 9 (V3 f. 3 a2), which has the highest S/N ratio, yields the ideal surface

Source	Degree of freedom (DOF)	The sum ofsquares (SS)	Adj(SS)	Adj(MS)	F	P-Value	Percentcontribution(PC) %	Remarks
V	z	96.84	96.S4	48.419	24.47	0.039	20	Sisnificant
F	2	149.7	149.7	74.865	37.84	0.026	32	Significant
A	**2**	218.7	218.7	109.33	55.25	0.018	46.6	Sisnificant
Residual error	2	3.957	3.957	1.979				
Total	8	469.191						

Table 6. ANOVA-Based Optimizations.

Experimental serial number	Cutting speed V (m/mm)	Feed rate f (mm/rev)	Cutting depth a (mm)	Tool wear Ymax Mean (μm)	Ymax S/N (μm)
1	80	0.05	0.2	227.089	−47.1239
2	80	0.10	0.4	201.712	−46.0946
3	80	0.15	0.6	232.031	−47.3109
4	100	0.05	0.4	195.657	−45.8299
5	100	0.10	0.6	209.539	−46.4253
6	100	0.15	0.2	170.286	−44.6236
7	120	0.05	0.6	215.970	−46.6879
8	120	0.10	0.2	143.500	−43.1370
9	120	0.15	0.4	142.375	−43.0687

Table 7. Experimental Results for Tool Insert Wear, Observed and Predicted Signal-to-Noise (S/N) Ratios for Tool Wear.

roughness parameters. The parameters for this experiment are V = 120 m/min, f = 0.15 mm/rev, and a = 0.4 mm. Table 8 lists the optimal parameters.

For each factor, the average signal-to-noise (S/N) ratio is calculated to prioritize the parameters based on their importance. Equations (8–10) provide a sample calculation for Factor V (cutting speed)[31]:

$$SNv_1 = (-47.1239 - 46.0946 - 47.3109)/3 = -46.84 \tag{8}$$

$$SNv_2 = (-45.8299 - 46.4253 - 44.6236)/3 = -45.63 \tag{9}$$

$$SNv_3 = (-46.6879 - 43.1370 - 43.0687)/3 = -44.30 \tag{10}$$

The range is calculated to assess the impact of this factor:

$$\Delta = SNV_{max.} - SNV_{min.} = -44.30 - (-46.84) = 2.54 \tag{11}$$

According to Table 9, the cutting speed parameter exhibits the largest variation among its levels in this study, leading to a significant impact on the experimental response (tool wear). In contrast, the feed rate parameter shows minimal influence on the same.

Esp. No	Process parameters	Tool wear (μn)
9	**V3 f. 3** m	142.**375**

Table 8. Optimal parameters of process.

Level	V	F	A
1	−46.84	−46.55	−44.96
2	−45.63	−45.22	−45.00
3	−44.30	−45.00	−46.81
Delta	2.54	1.55	1.85
Rank	1	3	2

Table 9. Signal-to-Noise (S/N) Response and Delta Value of Ymax for Each Parameter.

The variation for all parameters with signal-to-noise ratio is displayed in the following figure. The delta values of parameters V, f, and an are 2.54, 1.55, and 1.85, respectively, as indicated by Table 9. Figure 6 plots the delta value for every parameter[32–39].

From Fig. 7, it is shown that the tool wear value decreases with an increase in the cutting speed parameter and feed rate. Still, it decreases from level one to level two and then increases from level two to level three with increasing depth of cut. It is noticed that there is a long variation between the levels of each of the two parameters (cutting speed and depth of cut). Consequently, the two parameters occupy the first two affected parameters in the machining process. Therefore, the feed rate is the last affected parameter in the machining process.

Variance analysis (ANOVA)

ANOVA was applied to assess the impact of feed rate, cutting depth, and cutting speed on tool wear. The results, detailed in Table 10, are presented with a 95% confidence level. The findings indicate that cutting speed is the

Figure 6. Average Signal-to-Noise (S/N) Ratio for Ymax.

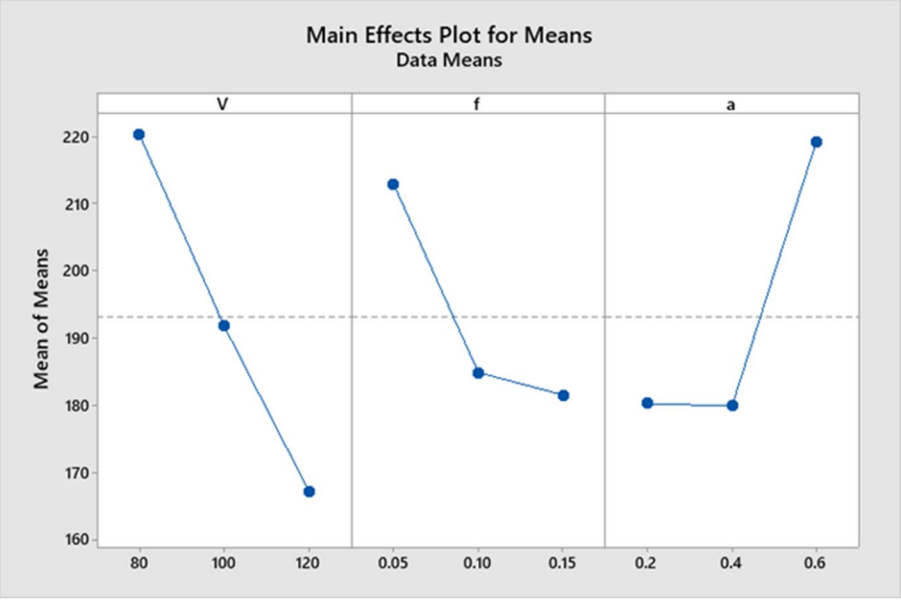

Figure 7. Main effects plot for Means.

Source	Degree of freedom (DOF)	The sum of squares (SS)	Adj (SS)	Adj (MS)	F	P-Value	Percent contribution (PC)%	Remarks
V	**2**	9.7240	9.7240	4.8620	43.55	0.022	46.7	Significant
F	**2**	4.2024	4.2024	2.1012	18.82	0.050	20.2	Significant
A	**2**	6.6882	6.6882	3.3441	29.95	0.032	32.1	Significant
Residual error	2	0.2233	0.2233	0.1116				
Total	8	20.8379						

Table 10. ANOVA-Based Optimization for Tool Wear.

most significant parameter, contributing 46.7% to tool insert wear. On the other hand, the feed rate is the least influential, accounting for a 32.1% contribution.

The mechanisms of Tool wear

The wear height of the tool for each experiment was measured using a scanning electron microscope (SEM) to optimize through the Taguchi method. This approach was utilized to analyze the complexity of tool wear during the turning of TC21, as detailed in Table 4. The scanned images from each experiment are displayed in Fig. 8. Among the parameters tested, cutting speed was found to have the most significant impact on tool wear during the turning experiments with TC21.

Comparison of the results between the initial and heat treated specimens

After accomplishing the trials for two stages (as received and as treated), it was noticed that the improvement of machinability after heat treatment. The surface roughness decreased from 0.16 to 0.07 μm with an improvement percentage of 56.25%, and the tool wear from 187.77 to 142.375 μm with an improvement percentage of 24.18%. The improvement will be shown in Fig. 9(a) and (b).

Although the increase in hardness after heat treatment from 34.8 to 50.33 HRC, the refinement of grain size in microstructure from (α + β) to (α + β) with secondary α platelets (αs) formed in residual β matrix as a result of forming secondary alpha platelets in beta matrix that leads to the increased volume fraction of beta phase as shown in Fig. 2(a,b) in section "Material and method", and by choosing an appropriate cutting tool insert (coated carbide) and select optimized cutting parameters, all these factors lead to improve the machinability after heat treatment.

Table 11 displays the comparison of the results between as-received and heat-treated samples. It is noticed from Table 11 the improvement of the two responses after applying the heat treatment process. The following bar charts as shown in Fig. 9 show the improvement that occurred after heat treatment in both responses (Surface roughness and tool wear).

Conclusions

The conclusions drawn from the surface roughness prediction model and the tool wear prediction model for TC21 Ti-alloy tool inserts are as follows:

1. Under optimal conditions, experiment no. 9 achieved the lowest surface roughness with the highest signal-to-noise ratio. The best machining parameters were V = 120 m/min, f = 0.15 mm/rev, and a = 0.4 mm, achieving a Ra of 0.07 μm.
2. Cutting depth is the most influential parameter on surface roughness, accounting for 46.6% of its variability.
3. Cutting speed has the least impact on surface roughness, contributing 20% to its variation.
4. For tool wear, experiment no. 9 also displayed the lowest levels under optimal conditions, again with the highest signal-to-noise ratio. The optimal machining parameters were the same as above, with a resultant tool wear measurement of Y = 142.375 μm.
5. The speed of cut is the most significant factor affecting tool insert wear, with a 46.7% contribution.
6. The feed rate, contributing 20.2% to the overall tool wear, is the least significant parameter.

In future work, we can consider other machining parameters besides the mentioned parameters. The considered machining parameters may be the consuming time, machining cost, the variety of cutting tool inserts, and cutting tool geometries (rake and clearance angle). Also, there are other things to be considered like machining conditions (dry, minimum quantity lubrication, nitrogen cooling, etc.) and achieving multi-heat treatment stages with temperature variations, and cooling rate (Furnace cooling, air cooling, and water quenching).

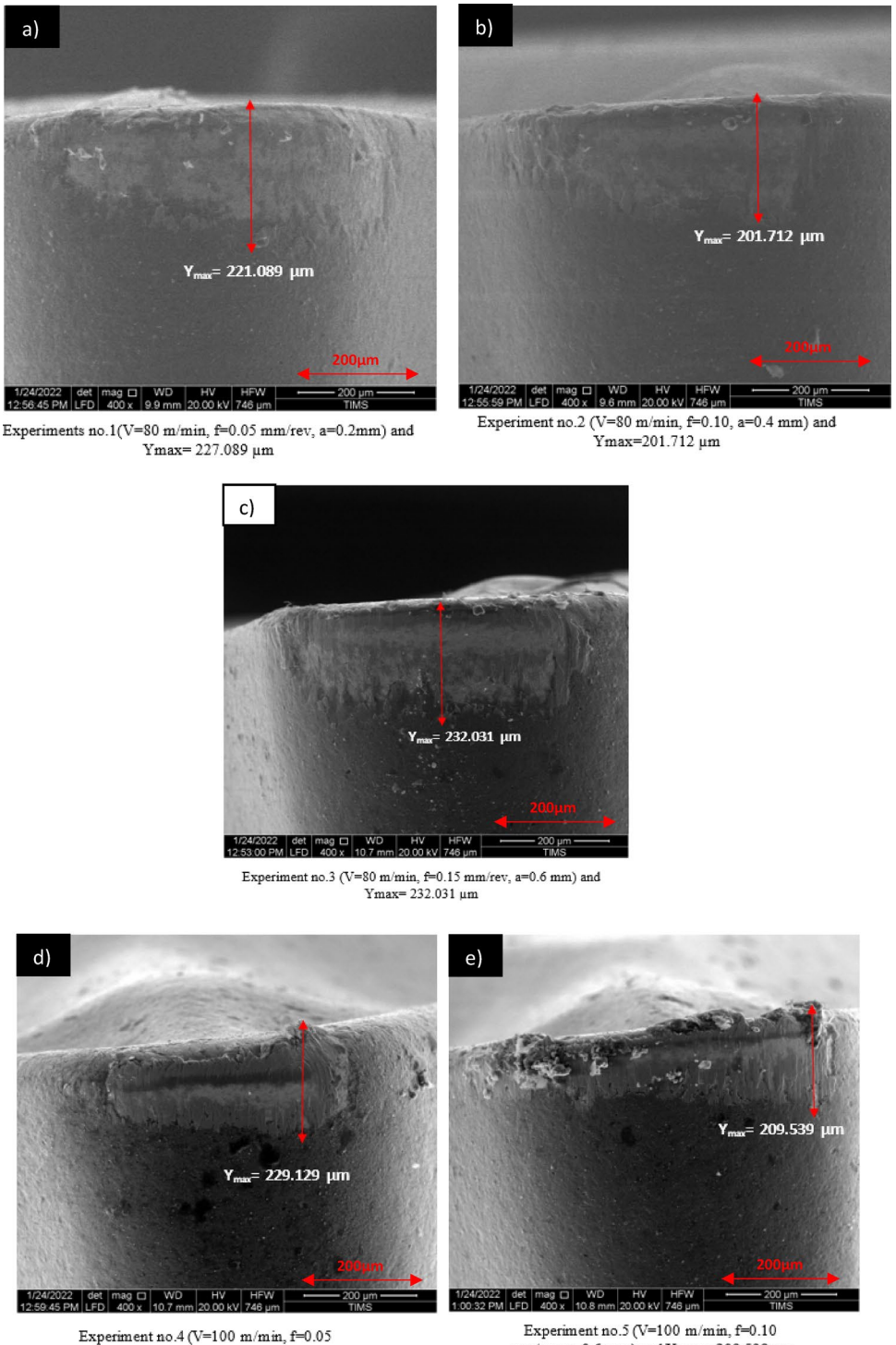

Experiments no.1(V=80 m/min, f=0.05 mm/rev, a=0.2mm) and Ymax= 227.089 µm

Experiment no.2 (V=80 m/min, f=0.10, a=0.4 mm) and Ymax=201.712 µm

Experiment no.3 (V=80 m/min, f=0.15 mm/rev, a=0.6 mm) and Ymax= 232.031 µm

Experiment no.4 (V=100 m/min, f=0.05 mm/rev, a=0.4 mm) and Ymax=229.129 µm

Experiment no.5 (V=100 m/min, f=0.10 mm/rev, a=0.6 mm) and Ymax=209.539 µm

Figure 8. SEM images of the wear of flank face.

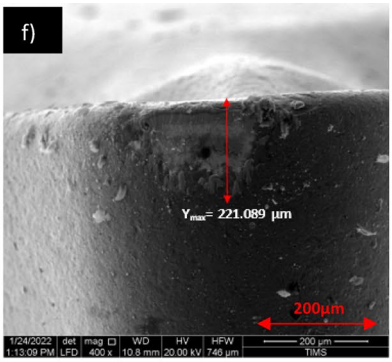

Experiment no.6 (V=100 m/min, f=0.15 mm/rev, a=0.2 mm) and Ymax= 170.286 µm [optimal experiment]

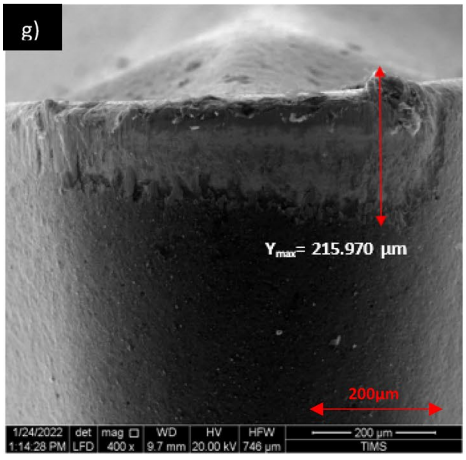

Experiment no.7 (V=120 m/min, f=0.05 mm/rev, a=0.6 mm) and Ymax=215.970 µm

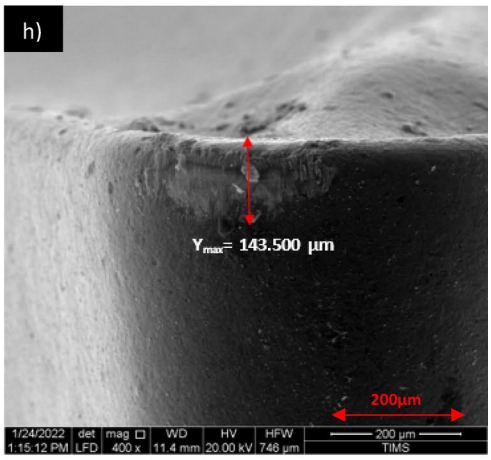

Experiment no.8 (V=120 m/min, f=0.10 mm/rev, a=0.2 mm) and Ymax=143.500 µm

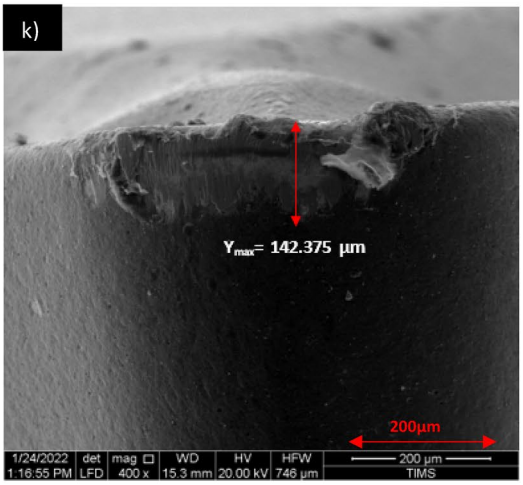

Experiment no.9 (V=120 m/min, f=0.15 mm/rev, a=0.4 mm) and Ymax=142.375 µm

Figure 8. (continued)

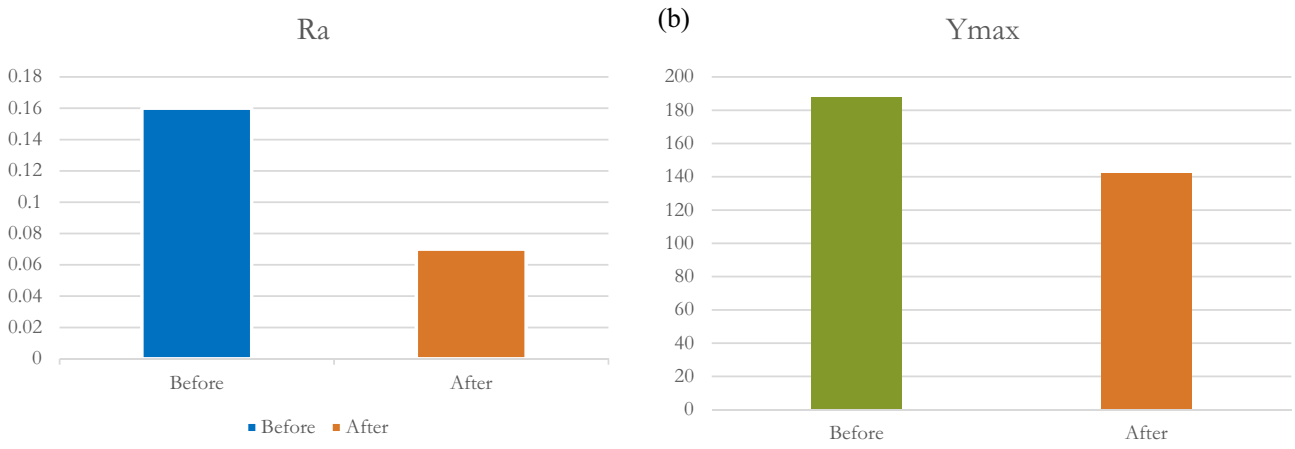

Figure 9. (**a**) Surface roughness improvement. (**b**) Tool wear improvement.

Results	Surface Roughness (Ra)		Tool wear (Y_{max})	
	As received	As treated	As received	As treated
Mean	0.16 µm[28]	0.07 µm	187.77 µm[28]	142.375 µm
S/N Ratio	15.917 µm	23.0983 µm	−45.4725 µm	−43.0687 µm
Prediction model	6.564%	8.76%	8.76%	7.47%
Improvement percentage	56.25%		24.18%	

Table 11. Comparison of the results between as-received and heat-treated samples.

Data availability

All data generated or analyzed during this study are included in this published article.

Received: 29 March 2024; Accepted: 24 June 2024
Published online: 17 July 2024

References

1. Khanna, N. & Kuldip, S. Machinability study of α/β and β titanium alloys in different heat treatment conditions. *Inst. Mech. Eng.* **227**(3), 357–361. https://doi.org/10.1177/0954405412469509 (2013).
2. Zhaoju, Z. & Sun, J. Investigation on the influence of tool wear upon chip morphology in end milling titanium alloy Ti6Al4V. *Int. J. Adv. Manuf. Technol.* **83**, 1477–1485. https://doi.org/10.1007/s00170-015-7690-1 (2016).
3. Balaji, J. H., Krisharaj, V. & Yogeswaraj, S. Investigation on the high-speed turning of titanium alloys. *Proc. Eng.* **64**, 926–935. https://doi.org/10.1016/j.proeng.2013.09.169 (2013).
4. Elshaer, R. N., El-Hadad, S. & Nofal, A. Influence of heat treatment processes on microstructure evolution, tensile and tribological properties of Ti6Al4V alloy. *Sci. Rep.* **13**(1), 11292 (2023).
5. Ahmed, F. S., El-Zomor, M. A., Abo Ghazala, M. S. & Elshaer, R. N. Influence of α-phase morphology on mechanical characteristics, cycle oxidation, and hot corrosion behavior of Ti-6Al-3Mo-2Nb-2Zr-2Sn-15 Cr Alloy. *Metallogr. Microstruct. Anal.* **11**(5), 1–15 (2022).
6. Ahmed, F. S., El-Zomor, M. A., Ghazala, M. S. A. & Elshaer, R. N. Effect of oxide layers formed by thermal oxidation on mechanical properties and NaCl-induced hot corrosion behavior of TC21 Ti-alloy. *Sci. Rep.* **12**(1), 19265 (2022).
7. Zhang, H., Zhao, J., Wang, F., Zhao, J. & Li, A. Cutting forces and tool failure in high-speed milling of titanium alloy TC21 with coated carbide tools. *Inst. Mech. Eng.* **229**(1), 20–27. https://doi.org/10.1177/0954405414526578 (2015).
8. Raut, Y. & Bhaskar,. Optimization of parameters to reduce the surface roughness in face milling operation on stainless steel and mild steel work piece applying Taguchi Method. *Int. J. Sci. Res. Eng. Trends.* **6**, 202–208. https://doi.org/10.14445/22315381/IJETT-V68I1P202 (2020).
9. Shahebrahimia, S. P. & Dadvandb, A. Optimization of cutting parameters for turning operation of titanium alloy Ti-6Al-4V material workpiece using the Taguchi method. *Adv. Mater. Res.* **685**, 57–62. https://doi.org/10.4028/www.scientific.net/AMR.685.57 (2013).
10. Özlü, B. & Akgün, M. Evaluation of the machinability performance of PH 13–8 Mo maraging steel used in the aerospace industry. *Proc. Inst. Mech. Eng. Part E J. Process Mech. Eng.* **238**(2), 687–699. https://doi.org/10.1177/09544089231216035 (2024).
11. Pei, L., Shu, X., (2020) Investigation of the turning process of the TC21 titanium alloy: Experimental analysis and 3D simulation. Institution mechanical engineers, China
12. Zhang, X. & Wu, H. Effect of tool angle on cutting force and residual stress in the oblique cutting of TC21 alloy. *Int. J. Adv. Manuf. Technol.* **98**, 791–797 (2018).
13. Özlü, B., Demir, H., Türkmen, M. & Gündüz, S. Examining the machinability of 38MnVS6 microalloyed steel, cooled in different mediums after hot forging with the coated carbide and ceramic tool. *J. Mech. Eng. Sci.* **235**(22), 6228–6239. https://doi.org/10.1177/0954406220984498 (2021).
14. Qian, X. & Duan, X. Effect of tool microstructure on machining of titanium alloy TC21 based on simulation and experiment. *Int. J. Adv. Manuf. Technol.* **111**, 2301–2309 (2020).

15. B Ã-Zlãœ,. Evaluation of energy consumption, cutting force, surface roughness and vibration in machining toolox 44 steel using taguchi-based gray relational analysis. *Surface Rev. Lett. (SRL)* **29**(08), 1–17. https://doi.org/10.1142/S0218625X22501037 (2022).
16. Ravi Kumara, S. M. & Kulkarnib, S. K. Analysis of hard machining of titanium alloy by Taguchi method. *Mater. Today* **4**, 10729–10738. https://doi.org/10.1016/j.matpr.2017.08.020 (2016).
17. John, D., Aslani, K. E., Fountas, N. A. & Nikolaos, M. A comparative investigation of Taguchi and full factorial design for machinability prediction in turning of a titanium alloy. *Measurement* https://doi.org/10.1016/j.measurement.2019.107213 (2019).
18. Abdelmoneim, A., Elshaer, R. N., El-Shennawy, M. & Sobh, A. S. Modeling of wear resistance for TC21 Ti-alloy using response surface methodology. *Sci. Rep.* **13**(1), 4624. https://doi.org/10.1038/s41598-023-31699-1 (2023).
19. Elshaer, R. N. Effect of initial α-phase morphology on microstructure, mechanical properties, and work-hardening instability during heat treatment of TC21 Ti-alloy. *Metallogr. Microstruct. Anal.* **11**(2), 1–16 (2022).
20. Qian, X. & Duan, X. Effect of tool microstructure on machining of titanium alloy TC21 based on simulation and experiment. *Int. J. Adv. Manuf. Techn.* **111**, 2301–2309. https://doi.org/10.1007/s00170-020-06248-z (2020).
21. Zhang, X. & Wu,. Effect of tool angle on cutting force and residual stress in the oblique cutting of TC21 alloy. *Int. J. Adv. Manuf. Technol.* **98**, 791–797. https://doi.org/10.1007/s00170-018-2324-z (2018).
22. Wu, H. & To, S. Serrated chip formation and their adiabatic analysis by using the constitutive model of titanium alloy in high -speed cutting. *J. Alloys Compounds* **629**, 368–373 (2015).
23. Wu, H. & Guo, L. Machinability of titanium alloy TC21 under orthogonal turning process. *Mater. Manuf. Processes* **29**, 1441–1445. https://doi.org/10.1080/10426914.2014.952023 (2014).
24. Li, M. *et al.* Research on surface integrity in graphene nanofluid MQL milling of TC21 alloy. *Int. J. Abras. Technol.* **9**(1), 49. https://doi.org/10.1504/IJAT.2019.10019131 (2019).
25. Akgün, M., Özlü, B. & Kara, F. Effect of PVD-TiN and CVD-Al2O3 coatings on cutting force, surface roughness, cutting power, and temperature in hard turning of AISI H13 Steel. *J. Mater. Eng. Perform.* **32**, 1390–1401. https://doi.org/10.1007/s11665-022-07190-9 (2023).
26. Guilin, L. Research on tool wearing on milling of TC21 titanium alloy. *IOP Conf. Ser.: Earth Environ. Sci.* **69**, 012118. https://doi.org/10.1088/1755-1315/69/1/012118 (2017).
27. Shi, Q., Li, L., He, N., Zhao, W. & Liu, X. Experimental study in high speed milling of titanium alloy TC21. *Int. J. Adv. Manuf. Technol.* **64**(1–4), 49–54. https://doi.org/10.1007/s00170-012-3997-3 (2012).
28. Sobh, A. S., Sayed, E. M., Barakat, A. F. & Elshaer, R. N. Turning parameters optimization for TC21 Ti-alloy using Taguchi technique. *J. Basic Appl. Sci.* https://doi.org/10.1186/s43088-023-00356-x (2023).
29. Sun, T. *et al.* Machinability of plunge milling for damage-tolerant titanium alloy TC21. *Int. J. Adv. Manuf. Technol.* **85**(5–8), 1315–1323. https://doi.org/10.1007/s00170-015-8022-1 (2015).
30. Zhang, L., Ji, X. & Sun, S. The study on high-speed turning parameters optimization of TC21 titanium alloy. *Academic journal of manufacturing engineering* **85**(5), 1315–1323 (2017).
31. Che-Haron, C. H. Tool life and surface integrity in turning titanium alloy. *Journal of Materials Processing Technology* **118**(1–3), 231–237 (2001).
32. Shahebrahimia, S. P. & Dadvandb, A. Optimization of cutting parameters for turning operation of titanium alloy Ti-6Al-4V material workpiece using the Taguchi method. *Adv. Mater. Res.* **685**, 57–62 (2013).
33. Hasçalık, A. & Çaydaş, U. Optimization of turning parameters for surface roughness and tool life based on the Taguchi method. *Int. J. Adv. Manuf. Technol.* **38**, 896–903 (2008).
34. Ravi Kumara, S. M. & Kulkarnib, S. K. Analysis of hard machining of titanium alloy by Taguchi method. *Mater. Today* **4**, 10729–10738 (2016).
35. Singaravel, B. & Selvaraj, T. Application of Taguchi method for optimization of parameters in turning operation. *J. Manuf. Sci. Prod.* **16**(3), 183–187 (2016).
36. Athreya, S. & Venkatesh, Y. D. Application of Taguchi method for optimization of process parameters in improving the surface roughness of lathe facing operation. *Int. Refereed J. Eng Sci* **3**, 13–19 (2012).
37. Abhang, L. B., Hameedullah, M. (2012) optimization of machining parameters in steel turning operation by Taguchi method. India 38, pp.40–48
38. Lin, Y.-C., Wang, A.-C., Wang, D.-A. & Chen, C.-C. Machining performance and optimizing machining parameters of Al_2O_3–TiC ceramics using EDM based on the Taguchi method. *Mater. Manuf. Processes* **24**, 667–674 (2009).
39. Elshaer, R. N., Ibrahim, K. M. & Farahat, A. I. Z. Worn surface topography and mathematical modeling of Ti-6Al-3Mo-2Sn-2Zr-2Nb-1.5 Cr alloy. *Sci. Rep.* **13**(1), 8878 (2023).

Author contributions

Conceptualization, R.N.E., E.M.S., A.F.B., A.A.E., and A.S.S.; methodology, R.N.E., and E.M.S.; validation, R.N.E., E.M.S., and A.F.B., ; formal analysis, R.N.E., E.M.S., and A.F.B., ; investigation, R.N.E., and E.M.S.; resources, R.N.E..; data curation, R.N.E., E.M.S., A.F.B., A.A.E., and A.S.S.; writing-original draft preparation, R.N.E. and E.M.S.; writing-review and editing, R.N.E., E.M.S., and A.F.B., ; visualization, R.N.E., E.M.S., A.F.B., A.A.E., and A.S.S.; supervision, R.N.E., E.M.S., and A.F.B., . All authors have read and agreed to the published version of the manuscript.

Funding

Open access funding provided by The Science, Technology & Innovation Funding Authority (STDF) in cooperation with The Egyptian Knowledge Bank (EKB).

Competing interests

The authors declare no competing interests.

Additional information

Correspondence and requests for materials should be addressed to R.N.E.

Reprints and permissions information is available at www.nature.com/reprints.

Publisher's note Springer Nature remains neutral with regard to jurisdictional claims in published maps and institutional affiliations.